

## ARTICLES

## Magnetic Field Control of Photoinduced Silver Nanoparticle Formation

J. C. Scaiano,<sup>\*,†</sup> Carolina Aliaga,<sup>†</sup> Steven Maguire,<sup>†</sup> and Dashan Wang<sup>‡</sup>*Department of Chemistry, University of Ottawa, Ottawa, Ontario K1N 6N5, Canada, and Institute for Chemical Process and Environmental Technology, National Research Council, Ottawa, Ontario K1A 0R6, Canada**Received: March 20, 2006; In Final Form: April 22, 2006*

The micellar photoreduction of benzophenone in the presence of  $\text{Ag}^+$  leads to very rapid and efficient formation of silver nanoparticles. External magnetic fields can be used to control the rate of formation and properties of silver nanoparticles generated by reaction of ketyl radicals formed in the photoreduction of benzophenone in surfactant micelles. The effect is attributed to Zeeman splitting of the triplet sublevels of the confined radical pair that causes a reduction in the rate of geminate processes and increases the availability of ketyl radicals (through escape processes) for metal ion reduction.

Silver nanoparticles can be readily produced by reductive processes in homogeneous or micellar solution or in polymer films<sup>1–4</sup> and characterized through the absorption of the plasmon band at  $\sim 420$  nm.<sup>5</sup> Ketyl radicals, produced in the photoreduction of ketones,<sup>6</sup> are excellent reducing agents and efficiently convert  $\text{Ag}^+$  to  $\text{Ag}^0$ .<sup>1,2,7,8</sup> The photoreduction of benzophenone is a convenient source of ketyl radicals; the anticipated mechanism in the presence of  $\text{Ag}^+$  involves electron transfer by ketyl radicals as illustrated in Scheme 1.

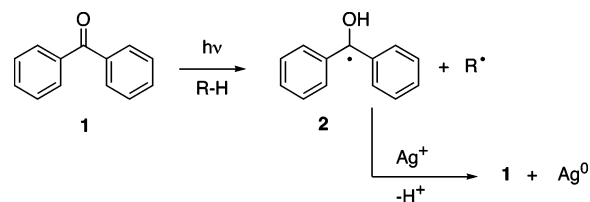
Photoreduction of ketones in micelles can provide confinement for radical pairs (RPs), and such confinement can be used to control the chemistry of the radicals; the RPs are normally generated as a triplet pair, reflecting the multiplicity of the reactive excited ketones.<sup>6,9</sup> The use of anionic micelles provides a convenient medium in which  $\text{Ag}^+$  salts, as well as hydrophobic reagents such as benzophenone (**1**, BP), and suitable hydrogen donors can be solubilized; further, surfactants can help stabilize the metal nanoparticles formed.<sup>4,10</sup>

In this work, we have prepared micelles of sodium dodecyl sulfate (SDS), and to promote the rapid generation of ketyl radicals,<sup>11,12</sup> we used 1,4-cyclohexadiene (CHD), an excellent hydrogen donor<sup>13</sup> whose behavior in micelles is well-understood.<sup>11,12</sup> Irradiation of BP in this system in the presence of  $\text{Ag}^+$  leads to its reduction<sup>1,2</sup> with rapid generation of the  $\text{Ag}^0$  plasmon band, according to the mechanism of Scheme 1, followed by  $\text{Ag}^0$  aggregation to yield nanoparticles.

## Experimental Section

**General.** Chemicals were purchased from Aldrich and used as received. Absorbance was measured using a Cary 50 Bio UV–visible spectrophotometer from Varian. Laser flash photolysis experiments were carried out in a customized Luzchem system using the third harmonic (355 nm) from Continuum Surelite laser for excitation.

## SCHEME 1: Photoreduction of Benzophenone Followed by Reduction of Silver Ions



**Sample Preparation.** Samples (3 mL) were prepared in Luzchem cuvettes made of UV grade fused silica, with a 10 mm optical path. A stock solution was prepared containing sodium dodecyl sulfate (SDS) and benzophenone at the desired concentrations. The silver perchlorate stock solution was added shortly before the experiment and the sample deaerated under a nitrogen flow. To avoid excessive foaming, the nitrogen flow was maintained above the solution (rather than bubbling) for 10–15 min, while the sample was simultaneously stirred by a vortex mixer. Once this procedure was complete, the required volume of pure 1,4-cyclohexadiene (highly volatile) was added with a microliter syringe and the sample stirred (vortex) for a few seconds and sealed with Parafilm.

**Magnetic Field Effects.** The UV–visible absorption spectrum of the samples, prepared as described above, was recorded and the sample exposed to UV light ( $> 320$  nm) with or without a magnetic field, using the setup shown in the Supporting Information. Immediately after exposure ( $< 10$  min), the UV–visible spectrum was recorded again, and the data used for plots such as that of Figure 2 in this paper (vide infra). Note that the spectra shown correspond to the difference between the spectrum after exposure minus that recorded before irradiation.

Magnetic field experiments were carried out with a home-built magnet capable of dc fields up to 0.12 T (1200 G). The excitation was provided by a 150 W xenon lamp filtered through a 320 nm cutoff filter; this ensures that benzophenone is the only absorbing species.

**Transmission Electron Microscopy (TEM).** TEM specimens were prepared immediately after the nanoparticles were

<sup>\*</sup> [tito@photo.chem.uottawa.ca](mailto:tito@photo.chem.uottawa.ca).<sup>†</sup> University of Ottawa.<sup>‡</sup> National Research Council.

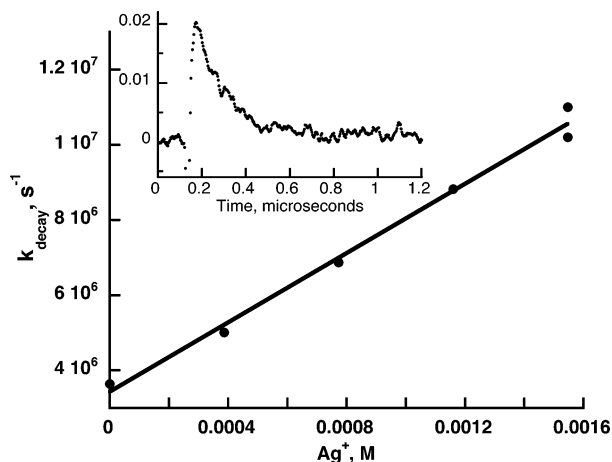


**Figure 1.** Quenching of the benzophenone triplet state in 0.1 M SDS (monitored at 600 nm to avoid ketyl radical interference) by  $\text{Ag}^+$ . The slope is the quenching rate constant and the intercept the reciprocal of the triplet lifetime. The inset shows the trace recorded for 0.77 mM  $\text{Ag}^+$ .

synthesized: 10  $\mu\text{L}$  of the solution was delivered with a microliter syringe onto a 300 mesh of copper grid coated with carbon film; the sample was washed with 25  $\mu\text{L}$  of methanol and allowed to dry in air. Washing reduces the amount of organic material and unreacted silver salts and improves TEM picture quality. TEM examination was carried out using a Philips CM20 STEM equipped with a Gatan UltraScan 1000 CCD camera and an energy-dispersive X-ray spectrometer (EDS), INCA Energy TEM 200. TEM was operated at 200 kV.

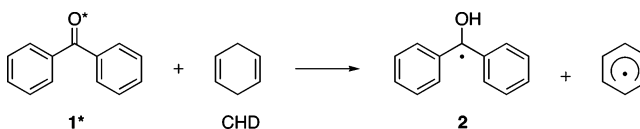
Bright field (BF) and high-resolution TEM (HRTEM) images were taken for particle size measurement and crystallographic determination. EDS was also used for composition analysis of the particles.

## Results and Discussion

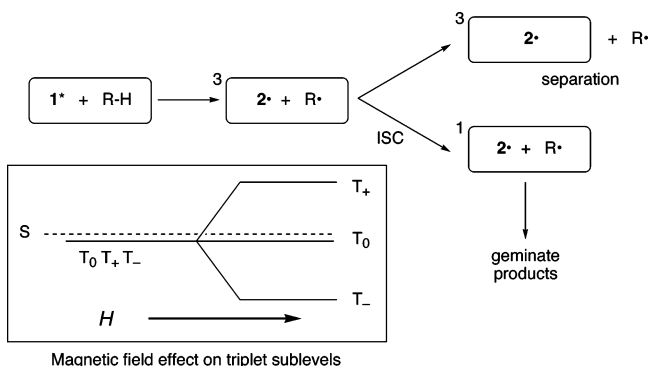
In order for the mechanism of Scheme 1 to be efficient, it is essential that the benzophenone triplets be quenched by the hydrogen donor, rather than by other species, notably,  $\text{Ag}^+$ . The rate constant for  $\text{Ag}^+$  quenching of benzophenone triplets was determined under our experimental conditions using laser flash photolysis techniques. The samples (BP in 0.1 M SDS solution under nitrogen) were excited at 355 nm to give the characteristic signal of the triplet state with  $\lambda_{\text{max}}$  at  $\sim 530$  nm. The decay of the BP triplet was monitored at 600 nm, where the signal is weaker than at 530 nm, but the absorption from ketyl radicals does not interfere;<sup>11</sup> a plot of the pseudo-first-order rate constant for triplet decay as a function of  $\text{Ag}^+$  concentration yields, from the slope, a triplet quenching rate constant by  $\text{Ag}^+$  of  $4.6 \times 10^9 \text{ M}^{-1} \text{ s}^{-1}$  and a triplet lifetime (at  $[\text{Ag}^+] = 0$ ) of ca. 290 ns (Figure 1); this short lifetime is controlled by triplet reaction with the surfactant.<sup>11</sup> The quenching by  $\text{Ag}^0$  may be assisted by Coulombic interactions (given the negative charge of the surfactant) and appears to be dynamic in nature, as judged by the fact that the decrease in lifetime upon addition of silver ions resulted in little or no change in the absorbance of triplet benzophenone immediately after the laser pulse, indicative of the absence of static quenching.

To facilitate hydrogen atom abstraction (rather than  $\text{Ag}^+$  quenching), we used 0.04 M CHD as a hydrogen donor; under these conditions, the lifetime of benzophenone triplets in SDS micelles is  $\sim 12$  ns, and hydrogen abstraction leading to ketyl radical formation is favored even in the presence of  $\text{Ag}^+$ . We estimate that in the presence of 0.01 M  $\text{Ag}^+$  about two-thirds

## SCHEME 2: Reaction of Benzophenone Triplets with 1,4-Cyclohexadiene.



## SCHEME 3: Separation of the RP Is Competitive with Intersystem Crossing; Application of an External DC Magnetic Field (inset box) Separates the Triplet Sublevels and Reduces the Probability for Geminate Reactions.



of the benzophenone triplets decay by reaction with CHD under our experimental conditions.

The initial radical pair (RP) produced by photoreduction of benzophenone is well-known to have triplet character (Schemes 2 and 3). Micelles provide RP confinement and increased opportunities (time) for geminate processes to occur, in the benzophenone system,<sup>11,12</sup> as well as in many other micellar systems involving RPs.<sup>14,15</sup> The RPs decay by a competition of geminate radical–radical reactions and escape from the micellar cage, as illustrated in Scheme 3 where the boxes represent micelles. Geminate reactions require a spin-flip, or intersystem crossing in the RP from the triplet (that cannot yield products), to the singlet RP that yields cage or geminate molecular products rapidly.<sup>11,12,15–17</sup> This competition can be controlled by application of external dc magnetic fields. The field ( $H$ ) causes Zeeman splitting of the triplet sublevels of the RP, as shown in the inset in Scheme 3.

In the presence of a magnetic field, the mechanism of Scheme 3 leads to a decrease in the efficiency of geminate RP processes from  $T_+$  and  $T_-$  that are no longer near-degenerate with the singlet RP ( $S$ ); RPs in  $T_+$  and  $T_-$  undergo intersystem crossing inefficiently or not at all, thus providing an opportunity for increased micellar escape, since the rate constant for micellar exit is not affected by external magnetic fields. Increased radical exit from the micelle favors competitive chemical processes, such as trapping by ions in the aqueous phase; the MF affects the radical decay, but not its absorption spectrum. The fields required for these effects are usually small ( $\leq 0.1$  T), since their role is simply to break the  $S$ – $T$  degeneracy.<sup>11,16</sup>

Upon UV ( $> 320$  nm, xenon lamp and filter) irradiation of BP/CHD/SDS containing 0.01 M  $\text{Ag}^+$ , one can readily detect the formation of the characteristic plasmon band, as shown in Figure 2. The band at ca. 330 nm is mostly due to the  $n, \pi^*$  absorption from BP. The formation of the plasmon band is linear with time, and peaks at 414 nm (vide infra). Formation of this absorption occurs in a remarkably short time; for comparison, earlier work under similar irradiation conditions involved exposure times about 100 times longer.<sup>1,8</sup> In our studies,  $\text{Ag}^+$  triplet quenching is minimized by a careful choice of the hydrogen donor.<sup>11,12</sup>

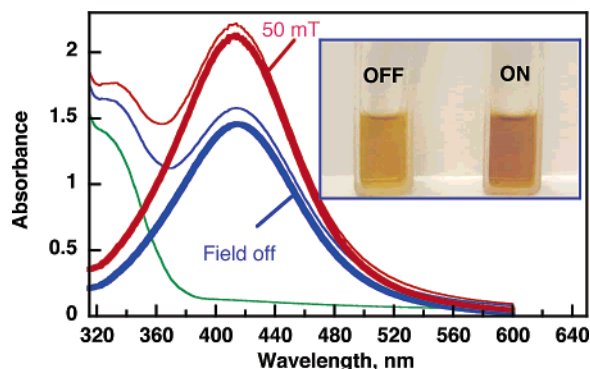


**Figure 2.** Formation of Ag nanoparticles after 30 s irradiation (BP 0.005 M, SDS 0.1 M,  $\text{Ag}^+ = 0.01$  and 0.04 M CHD) in the absence (blue) and presence (red) of a 50 mT magnetic field. The thick lines are the subtraction of the actual spectrum recorded (thin lines) minus the preirradiation spectrum (green). The insert shows samples irradiated for 30 s with and without an applied magnetic field.

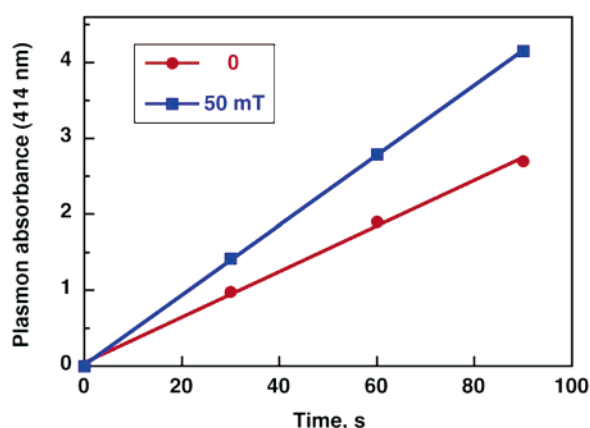


**Figure 3.** Formation of silver nanoparticles during UV irradiation in the absence (red) and presence (blue) of a 50 mT magnetic field (BP 0.005 M, SDS 0.1 M,  $\text{Ag}^+ = 0.01$  and 0.04 M CHD). Absorbance values above 3 have considerable ( $> 10\%$ ) error even if coincidentally they fit perfectly on the line.

When  $\text{Ag}^+$  is present, the effect of the external field increases the aqueous availability of ketyl radicals to reduce the metal ion and induce a large increase in the rate of formation of nanoparticles as deduced by the observation of the plasmon band at 414 nm, typical of spherical nanoparticles.<sup>18</sup> The changes caused by magnetic fields are readily observable, as seen in the photographs inserted in Figure 2 and in Figure 3. The results suggest that  $\text{Ag}^+$  ions trap predominantly ketyl radicals after they escape from the micelle. It should be noted that it is unimportant which radical leaves the micelle first (the cyclohexadienyl radical probably does); once the geminate character of the RP has been lost, the remaining radical has abundant opportunity (time) to escape, since there is little that these radicals can do, other than exit, when they are single micelle occupants.

The effect of the magnetic field occurs at relatively low fields and appears to saturate at around 0.1 T, as shown in Figure 4. In the plateau region, we see a 67% signal increase; for comparison, when the RP separation is measured (without  $\text{Ag}^+$ ) the increase is 69%,<sup>11</sup> supporting the idea that both phenomena are based on the same primary processes, i.e., that magnetic fields promote radical separation as a result of Zeeman splitting of the triplet sublevels.

In the absence of CHD, Ag nanoparticles are also formed, but their formation is slower, with the plasmon band somewhat broader and less stable, as indicated by its evolution (over a

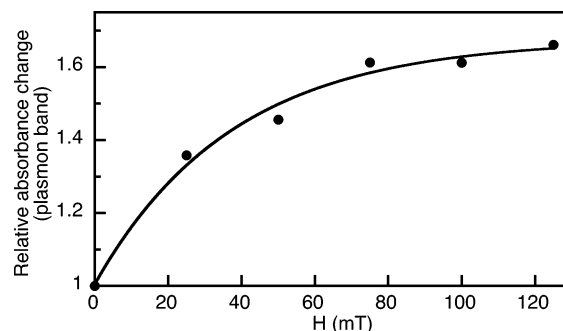


**Figure 4.** Magnetic field effect on the formation of silver nanoparticles during UV irradiation. (BP 0.005 M, SDS 0.1 M,  $\text{Ag}^+ = 0.01$  and 0.04 M CHD, 30 s exposure). Approximately 50% of the maximum effect is achieved with ca. 27 mT.

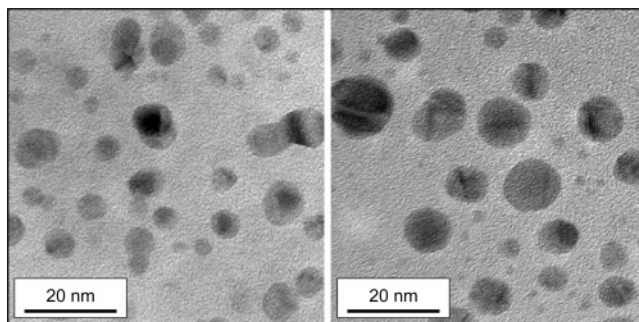


**Figure 5.** TEM photos recorded in samples containing CHD. The TEM sample was prepared within 10 min following UV exposure. The sample on the left was exposed for 90 s with no field, and the right one at 50 mT. The abundance of particles does not reflect the true abundance in the samples, but rather the selection of a TEM display area, where size is representative of the bulk.

few hours) to a much broader band, indicative of further aggregation. The results reflect that in the absence of CHD the lifetime of excited triplet benzophenone is ca. 300 ns,<sup>11</sup> making it an easy target for quenching by  $\text{Ag}^+$  ions (see Figure 1). Interestingly, the growth of the plasmon band under these conditions is almost twice as fast with 0.005 M  $\text{Ag}^+$ , compared with 0.01 M (note reversal); thus, at both concentrations, scavenging of ketyl radicals is efficient, and increased  $\text{Ag}^+$  concentration simply quenches more benzophenone triplet states,<sup>8</sup> thus limiting the ketyl radical generation.

It should be noted that  $\text{Ag}^+$  is well-known to form complexes with many alkenes,<sup>19</sup> including CHD.<sup>20</sup> At the concentrations used in this work, only a small fraction of the  $\text{Ag}^+$  will be complexed with CHD (given the modest equilibrium constant),<sup>20</sup> and thus, we do not expect a significant effect on the rate or mechanism for silver atom formation. However, we see increased particle stability in the presence of CHD, suggesting that the alkene may play a role in assisting nucleation and nanoparticle formation. Stabilization of silver clusters by alkenes is known,<sup>21,22</sup> although their role at the concentration used (0.04 M) is surprising;<sup>22</sup> it is possible that the SDS micelles home the growing nanoparticles and also provide a high local concentration for CHD.

TEM analysis of the nanoparticles (Figure 5) reveal particles with an average size 4–5 nm in the absence of a field; larger particles are multicrystalline and probably reflect aggregation of the smaller nanoparticles. In the presence of a field, the particles appear to be somewhat larger, typically ~8 nm. Aged samples (e.g., 2 h under nitrogen) show clear signs of particle aggregation, with complex networks (see Supporting Information) readily detectable by TEM and reminiscent of those

observed elsewhere.<sup>4</sup> This initial (ca. 2 h) aggregation does not lead to significant change in the shape of the plasmon band; eventually (days) the visible absorption shifts and broadens (see Supporting Information); this process is accelerated if air is allowed in the samples.

The reaction and the field effects are best observed when the samples are irradiated under a nitrogen atmosphere. However, even under air, the effect is readily observable, albeit the magnitude of the changes is reduced, and the particles are less stable. Oxygen is a well-known quencher of excited triplet states, as well as a free radical scavenger.<sup>23</sup> In the system under study, the short lifetime of the benzophenone triplet, the efficient scavenging of the ketyl radicals by  $\text{Ag}^+$ , and the rather low solubility of oxygen in water all combine to allow a good fraction of the reaction to proceed even under air.

Given that particles formed in the presence of a field are somewhat larger, and these are known to have a larger absorbance cross-section,<sup>24</sup> one may wonder if the difference in absorbance caused by a magnetic field (Figures 2 and 3) can be solely the result of having different nanoparticle sizes (rather than different  $\text{Ag}^0$  yields). However, particle absorbance increases roughly linearly<sup>24</sup> with their diameter, while the number of atoms grows with the cube of the particle size; therefore, the absorbance per gram-atom of silver actually decreases with increasing particle size. Thus, in terms of the yield of atomic silver, the nanoparticle size effect (larger particles in the presence of a magnetic field) would be to attenuate to some extent the observable magnetic field effect.

Attempts to detect the time-resolved growth of the plasmon band by laser flash photolysis failed, probably because growth at nucleation centers occurs beyond the millisecond window observable in our instrument. Formation of the plasmon band was readily observable in longer time scales (seconds and several laser pulses) under 355 nm laser irradiation.

In conclusion, magnetic field effects on ketone photoreduction in micelles can be used to control silver nanoparticle synthesis under mild conditions. The method provides spatial and temporal control for particle formation. External weak magnetic fields, add a new methodology for the manipulation of nanoparticle synthesis. Similar magnetic field control will probably apply to other metals and alloys; interestingly, significant effects occur in the range of commonly employed magnetic stirring bars ( $\leq 10$  mT).

**Acknowledgment.** J.C.S. is grateful to Natural Sciences and Engineering Research Council of Canada and the Province of Ontario Premier's program for generous support.

**Supporting Information Available:** Experimental methods, TEM aggregation data, nanoparticle formation kinetics, and stability information. This material is available free of charge via the Internet at <http://pubs.acs.org>.

## References and Notes

- (1) Eustis, S.; Krylova, G.; Eremenko, A.; Smirnova, N.; Schilla, A. W.; El-Sayed, M. *Photochem. Photobiol. Sci.* **2005**, *4*, 154.
- (2) Yonezawa, Y.; Sato, T.; Kuroda, S.; Kuge, K. *J. Chem. Soc., Faraday Trans.* **1991**, *87* (12), 1905.
- (3) Korchev, A. S.; Bozack, M. J.; Slaten, B. L.; Mills, G. *J. Am. Chem. Soc.* **2004**, *126* (1), 10. Evanoff, D. D., Jr.; Chumanov, G. *J. Phys. Chem. B* **2004**, *108*, 13948. Korchev, A. S.; Shulyak, T. S.; Slaten, B. L.; Gale, W. F.; Mills, G. *J. Phys. Chem. B* **2005**, *109* (16), 7733.
- (4) Pileni, M. P. *J. Phys. Chem. B* **2001**, *105* (17), 3358.
- (5) Burda, C.; Chen, X.; Narayanan, R.; El-Sayed, M. A. *Chem. Rev.* **2005**, *105* (4), 1025.
- (6) Scaiano, J. C. *J. Photochem.* **1973/74**, *2*, 81.
- (7) Sato, T.; Onaka, H.; Yonezawa, Y. *J. Photochem. Photobiol., A* **1999**, *127*, 83.
- (8) Kometani, N.; Doi, H.; Asami, K.; Yonezawa, Y. *Phys. Chem. Chem. Phys.* **2002**, *4*, 5142.
- (9) Turro, N. J. *Modern Molecular Photochemistry*; Benjamin/Cummings Publishing Co.: Menlo Park, 1978; p 628.
- (10) Maillard, M.; Pileni, M. P.; Link, S.; El-Sayed, M. A. *J. Phys. Chem. B* **2004**, *108* (17), 5230.
- (11) Scaiano, J. C.; Abuin, E. B.; Stewart, L. C. *J. Am. Chem. Soc.* **1982**, *104* (21), 5673.
- (12) Scaiano, J. C.; Abuin, E. B. *Chem. Phys. Lett.* **1981**, *81*, 209.
- (13) Paul, H.; Small, R. D., Jr.; Scaiano, J. C. *J. Am. Chem. Soc.* **1978**, *100*, 4520.
- (14) Turro, N. J. *Chem. Commun.* **2002**, 2279. Turro, N. J.; Garcia-Garibay, M. *Thinking Topologically about Photochemistry in Constrained Spaces. In Photochemistry in Organized and Constrained Media*; Ramamurthy, V., Ed.; VCH Publishers: New York, 1991; p 1.
- (15) Turro, N. J.; Grätzel, M.; Braun, A. M. *Angew. Chem., Int. Ed. Engl.* **1980**, *19*, 675.
- (16) Turro, N. J.; Kraeutler, B. *J. Am. Chem. Soc.* **1978**, *100*, 7432. Nagakura, S.; Hayashi, H. *Int. J. Quantum Chem.* **1984**, *18*, 571.
- (17) Kleinman, M. H.; Shevchenko, T.; Bohne, C. *Photochem. Photobiol.* **1998**, *67* (2), 198.
- (18) Mock, J. J.; Barbic, M.; Smith, D. R.; Schultz, D. A.; Schultz, S. *J. Chem. Phys.* **2002**, *116* (15), 6755.
- (19) Hartley, F. R. *Chem. Rev.* **1973**, *73* (2), 163.
- (20) Muhs, M. A.; Weiss, F. T. *J. Am. Chem. Soc.* **1962**, *84* (24), 4697.
- (21) Andrews, M. P.; Ozin, G. A. *J. Phys. Chem.* **1986**, *90* (13), 2923.
- (22) Andrews, M. P.; Ozin, G. A. *J. Phys. Chem.* **1986**, *90* (13), 2929.
- (23) Maillard, B.; Ingold, K. U.; Scaiano, J. C. *J. Am. Chem. Soc.* **1983**, *105* (15), 5095.
- (24) Evanoff, D. D., Jr.; Chumanov, G. *J. Phys. Chem. B* **2004**, *108* (37), 13957.